STABILITY OF BEDLOAD-DOMINATED ALLUVIAL DELTAS

Adichai PORNPROMMIN[1], Norihiro IZUMI[2], and Tetsuro TSUJIMOTO[3]

[1] Student Member of JSCE, Postgraduate Student, Dept. of Civil Engineering, Nagoya University (Furo-cho, Chikusa-ku, Nagoya 464-8603, Japan)

[2]Member of JSCE, Ph.D., Associate Professor, Dept. of Civil Engineering, Tohoku University

[3]Member of JSCE, Dr. of Eng., Professor, Dept. of Geo- & Environmental Engineering, Nagoya University

A linear stability analysis of the channel inception on bedload-dominated alluvial deltas is performed with the use of the shallow-water equations and the Exner equation. At the downstream end of a delta i.e. the delta front, there is a body of standing water, where water surface elevation of the water body controls the flow depth at the delta front. The bedload transported beyond the front is accumulated on the slope at the front, which causes the migration of the delta front. Upward-concave bed profile is found in the one-dimensional base state. In the two-dimensional linear stability analysis, only negative growth rate is found in all the cases. The absolute value of the growth rate increases with increasing the height of delta front, which implies that deltas with smaller height of delta front are more stable. It is concluded that bedload-dominated alluvial deltas are always stable. This result corresponds to the fact that fan deltas are formed if sediment is sufficiently coarse so that bedload is predominant.

Key Words: *alluvial deltas, channelization, linear analysis, downstream-driven theory, bedload*

1. INTRODUCTION

A *delta* is defined as an accumulation built by a terrestrial feeder system into or against a body of standing water such as a lake or sea. In a broad manner, deltas can be separated into alluvial deltas such as river delta and alluvial-fan delta, and non-alluvial delta such as pyroclastic delta and lava delta (Nemec[1] 1990). Only the alluvial deltas are in the scope of this study.

Under various situations, alluvial deltas form themselves differently, which has been intensively investigated by many geologists. In addition, there is a large amount of study by hydraulic engineers because sediment deposition around river mouths is an important subject from engineering viewpoints. Deltas also play important roles for the environment because of its unique ecological resources. For example, river delta provides abundant natural conditions, resulting in the habitation for a variety of creatures such as terrestrial animals, aquatic animals and plants.

It is found that grain size fraction is a basic terminology for the delta classification. Medium-size, radial deep-sea fans in western Mediterranean, Californian borderland and Alaska are found to be sand-dominated, while most of large-size, elongate ones such as Mississippi fan, Amazon, and Bengal are mud-dominated (Table 2 in Einsele[2] 1996). Therefore, suspended load might play an important role of this differentiation. This motivates us to investigate the characteristics of deltas in terms of processes of sediment transport. In this study, only bedload is taken into consideration as a first step for the investigation so that the phenomenon of bedload-dominated alluvial delta is well presented by the model.

The evolution of incipient channelization of the various types of geomorphology has been investigated recently. Izumi and Parker[3] (2000) performed a linear stability analysis to study incipient channelization on hillslopes composed of cohesive soil. Dey, Kitamura and Tsujimoto[4] (2001) studied the erosional process of headcut by experiments and numerical calculation. Izumi[5] (2001) performed a linear stability analysis to investigate the formation of submarine canyons.

Most of the previous analyses have dealt with channelization in erosional processes. In this study, a depositional process is studied in a bedload dominated case. After a one-dimensional base state solution is obtained, a two-dimensional linear stability analysis is performed to obtain the growth rate of the evolution of incipient channelization.

2. FORMULATION

(1) Governing equations

Let us consider the flow on the alluvial delta connecting to a large water body at its downstream end. **Fig. 1** shows our model configuration. We assume that the bed consists of non-cohesive sediment which is transported as only bedload. When the transported sediment get across the delta front, it is assumed to settle down on the slope at the front, causing the migration of the delta. If the water depth of the standing water is sufficiently large compared with the flow depth, wave impact is insignificant (Nemec[1] 1990). So, we neglect the effects of wave and tide in this study. Since the present analysis is devoted to the description of the depositional surface evolving in response to sheet flow, it motivates us to apply the St Venant shallow water equations, which can be described by the following equations:

$$\tilde{u}\frac{\partial \tilde{u}}{\partial \tilde{x}}+\tilde{v}\frac{\partial \tilde{u}}{\partial \tilde{y}}=-g\frac{\partial \tilde{h}}{\partial \tilde{x}}-g\frac{\partial \tilde{z}}{\partial \tilde{x}}-\frac{\tilde{\tau}_x}{\rho \tilde{h}} \tag{1}$$

$$\tilde{u}\frac{\partial \tilde{v}}{\partial \tilde{x}}+\tilde{v}\frac{\partial \tilde{v}}{\partial \tilde{y}}=-g\frac{\partial \tilde{h}}{\partial \tilde{y}}-g\frac{\partial \tilde{z}}{\partial \tilde{y}}-\frac{\tilde{\tau}_y}{\rho \tilde{h}} \tag{2}$$

$$\frac{\partial \tilde{u}\tilde{h}}{\partial \tilde{x}}+\frac{\partial \tilde{v}\tilde{h}}{\partial \tilde{y}}=0 \tag{3}$$

where tilde means the dimensional variables, $\tilde{x}$ and $\tilde{y}$ are the streamwise and lateral coordinates respectively, $\tilde{u}$ and $\tilde{v}$ are the $\tilde{x}$ and $\tilde{y}$ components of velocity respectively, $\tilde{h}$ and $\tilde{z}$ are the flow depth and the bed elevation respectively, $\tilde{\tau}_x$ and $\tilde{\tau}_y$ are the $\tilde{x}$ and $\tilde{y}$ components of bed shear stress respectively, ρ is the water density, and g is the gravity acceleration.

The bed shear stress vector $(\tilde{\tau}_x,\tilde{\tau}_y)$ is written as

$$(\tilde{\tau}_x,\tilde{\tau}_y)=\rho C_f\left(\tilde{u}^2+\tilde{v}^2\right)^{\frac{1}{2}}(\tilde{u},\tilde{v}) \tag{4}$$

where C_f is a friction coefficient and assumed to be a constant for simplicity in this study.

Time variation of bed elevation can be expressed by the following Exner equation:

$$\frac{\partial \tilde{z}}{\partial \tilde{t}}=-\frac{1}{1-\lambda_p}\left(\frac{\partial \tilde{q}_x}{\partial \tilde{x}}+\frac{\partial \tilde{q}_y}{\partial \tilde{y}}\right) \tag{5}$$

where λ_p is porosity, $\tilde{q}_x$ and $\tilde{q}_y$ are the $\tilde{x}$ and $\tilde{y}$ components of bedload transport rate, which is expressed as

$$(\tilde{q}_x,\tilde{q}_y)=\tilde{q}\left(\tilde{u}^2+\tilde{v}^2\right)^{-\frac{1}{2}}(\tilde{u},\tilde{v}) \tag{6}$$

where $\tilde{q}$ is the absolute value of bedload transport rate. When we employ the Meyer-Peter & Müller formula, it is expressed as

$$\tilde{q}=8\left(\tau^*-\tau_c^*\right)^{\frac{3}{2}}\left(R_s g\tilde{d}_s\right)^{\frac{1}{2}}\tilde{d}_s \tag{7}$$

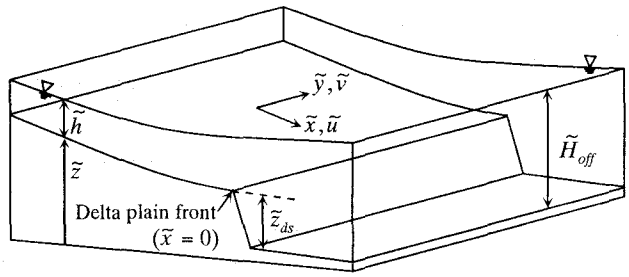

Fig. 1 The model configuration of the alluvial delta.

where R_s is the submerged specific gravity and $\tilde{d}_s$ is the sediment diameter.

When the Shields stress τ^* is much larger than the critical Shield stress τ_c^*, the above equation is further simplified as

$$\tilde{q}=8\tau^{*3/2}\left(R_s g\tilde{d}_s\right)^{\frac{1}{2}}\tilde{d}_s \tag{8}$$

This analysis is a first step to investigate the instability of the alluvial delta, so the understanding of the basic mechanism of the problem is a top priority. The simple form of (8) is used in this paper.

(2) Alluvial delta migration

If there is a constant sediment supply from the upstream, there occurs a constant deposition at the downstream end of the delta, which causes the migration of the delta front at a constant speed. The migration speed $\tilde{\sigma}$ is expressed as

$$\tilde{\sigma}=\frac{\tilde{q}_x\big|_{\tilde{x}=0}}{\left(1-\lambda_p\right)\tilde{z}_{ds}} \tag{9}$$

where $\tilde{z}_{ds}$ is the elevation at the delta front, which also can be assumed constant.

We assume this idealistic base state in order to perform a formal instability analysis so that the base state solution cannot be directly applied to real deltas. However, the model is expected to describe the essential characteristics of the phenomena qualitatively. Moreover, the self-preserving longitudinal profiles of one-dimensional delta have been observed experimentally by Izumi & Ikeda[6].

In the case that the alluvial delta is migrating in the streamwise direction at a constant speed $\tilde{\sigma}$, it is convinient to introduce the coordinates moving with the delta as follows:

$$\tilde{x}^*=\tilde{x}-\tilde{\sigma}\tilde{t},\quad \tilde{t}^*=\tilde{t} \tag{10a,b}$$

where the asterisk indicates the moving coordinates.

When the curvature radius in the two-dimensional case is sufficiently large, the circular shape of delta front can be approximated to be linear with enough accuracy. Thus, with the use of above relations, the Exner equation (5) is rewritten as

$$\frac{\partial \tilde{z}}{\partial \tilde{t}^*}-\tilde{\sigma}\frac{\partial \tilde{z}}{\partial \tilde{x}^*}=-\frac{1}{1-\lambda_p}\left(\frac{\partial \tilde{q}_x}{\partial \tilde{x}^*}+\frac{\partial \tilde{q}_y}{\partial \tilde{y}}\right) \tag{11}$$

(3) Normalization

The following transformations are introduced in order to nondimensionalize all the variables:

$$(\tilde{x}^*, \tilde{y}) = \frac{\tilde{H}_c}{C_f}(x, y),\ (\tilde{u}, \tilde{v}) = \tilde{U}_c(u, v) \quad (12a,b)$$

$$(\tilde{h}, \tilde{z}) = \tilde{H}_c(h, z),\ \tilde{t}^* = \frac{(1-\lambda_p)\tilde{H}_c^2}{C_f \tilde{Q}_c} t \quad (12c,d)$$

$$\tilde{\sigma} = \frac{\tilde{Q}_c}{(1-\lambda_p)\tilde{H}_c} \sigma \quad (12e)$$

where $\tilde{U}_c$, $\tilde{H}_c$ and $\tilde{Q}_c$ denote the flow velocity, flow depth and bedload corresponding to the Froude-critical flow condition, which are expressed as

$$\tilde{U}_c = (\tilde{q}_w g)^{1/3},\ \tilde{H}_c = \left(\frac{\tilde{q}_w^2}{g}\right)^{1/3} \quad (13a,b)$$

$$\tilde{Q}_c = 8\left(\frac{C_f \tilde{U}_c^2}{R_s g \tilde{d}_s}\right)^{3/2} \left(R_s g \tilde{d}_s^3\right)^{1/2} \quad (13c)$$

where $\tilde{q}_w$ is flow discharge per unit width.

Introducing Eqs.(12*a-e*) into Eqs.(1)-(3) and (11) and reducing, the following normalized equations are obtained:

$$u\frac{\partial u}{\partial x} + v\frac{\partial u}{\partial y} = -\frac{\partial h}{\partial x} - \frac{\partial z}{\partial x} - \frac{\left(u^2+v^2\right)^{\frac{1}{2}}}{h} u \quad (14)$$

$$u\frac{\partial v}{\partial x} + v\frac{\partial v}{\partial y} = -\frac{\partial h}{\partial y} - \frac{\partial z}{\partial y} - \frac{\left(u^2+v^2\right)^{\frac{1}{2}}}{h} v \quad (15)$$

$$\frac{\partial uh}{\partial x} + \frac{\partial vh}{\partial y} = 0 \quad (16)$$

$$\frac{\partial z}{\partial t} - \sigma\frac{\partial z}{\partial x} + \frac{\partial u^3}{\partial x} + \frac{\partial u^2 v}{\partial y} = 0 \quad (17)$$

3. THE ONE-DIMENSIONAL BASE STATE

(1) Governing equations

When the flow is assumed to be steady and uniform in the lateral direction, the time derivative terms and the terms associated with the lateral direction are dropped; thus, the governing equations reduce

$$u\frac{\partial u}{\partial x} + \frac{\partial h}{\partial x} + \frac{\partial z}{\partial x} + \frac{u^2}{h} = 0 \quad (18)$$

$$uh = 1 \quad (19)$$

$$-\sigma\frac{\partial z}{\partial x} + \frac{\partial u^3}{\partial x} = 0 \quad (20)$$

After some manipulation, Eqs.(18)-(20) yield the following differential equations:

$$\frac{du}{dx} = \frac{-u^3}{u - u^{-2} + 3u^2/\sigma} \quad (21)$$

Table 1 The parameters using in the analysis.

Description	unit	Case 1	Case 2
Water discharge, q_w	m^2/s	1	
Offshore water depth, H_{off}	m	5	10
Delta front elevation, z_{ds}	m	4	9
Sediment diameter, d_s	mm	1	

$$\frac{dh}{dx} = \frac{h}{3/\sigma + h - h^4} \quad (22)$$

$$\frac{dz}{dx} = \frac{1}{\sigma}\frac{du^3}{dx} \quad (23)$$

In order to solve Eqs.(21)-(23), we employ the downstream boundary condition that water surface is continuous at the interface between the river flow and the standing water body. When the depth of the standing water body is much larger than the flow depth, the downstream boundary condition is controlled by the water elevation of the water body, and the non-dimensional downstream flow velocity can be expressed as

$$u_{ds} = \frac{\tilde{q}_w}{\tilde{U}_c(\tilde{H}_{off} - \tilde{z}_{ds})} \quad \text{at} \quad x = 0 \quad (24)$$

Since the equations (21)-(23) cannot be reduced to be simple forms of exact solutions, we employ the expansion method using the non-dimensional migration speed $\sigma = u_{ds}^3 / z_{ds}$ as a small parameter. The second order approximation is the following:

$$u = u_{ds} - \frac{\sigma}{3}u_{ds}x + \frac{\sigma^2}{9}\left\{\left(1 - \frac{1}{u_{ds}^3}\right)x + \frac{u_{ds}}{2}x^2\right\} + O(\sigma^3) \quad (25)$$

$$h = h_{ds} + \frac{\sigma}{3}h_{ds}x + \frac{\sigma^2}{9}\left\{\left(h_{ds}^5 - h_{ds}^2\right)x + \frac{h_{ds}}{2}x^2\right\} + O(\sigma^3) \quad (26)$$

$$z = z_{ds} - u_{ds}^3 x + \sigma\left\{\frac{1}{3}\left(u_{ds}^2 - \frac{1}{u_{ds}}\right)x + \frac{u_{ds}^3}{2}x^2\right\}$$
$$+\sigma^2\left\{\frac{1}{9}\left(\frac{2}{u_{ds}^2} - \frac{1}{u_{ds}^5} - u_{ds}\right)x + \frac{1}{18}\left(\frac{2}{u_{ds}} - 5u_{ds}^2\right)x^2 - \frac{u_{ds}^3 x^3}{6}\right\} + O(\sigma^3) \quad (27)$$

where u_{ds} and z_{ds} are the non-dimensional flow velocity and bed elevation corresponding to the downstream condition, respectively.

(2) Solutions of the base state

The variables in **Table 1** are applied in order to examine the one-dimensional base state solutions. The difference between Cases 1 and 2 is the delta front elevation $\tilde{z}_{ds}$ which provides the variation of the migration speeds. The migration speed $\tilde{\sigma}$ in Case 1 equals to $21*10^{-5}$ m/s, while $\tilde{\sigma}$ in Case 2 give a small value and equals to $9*10^{-5}$ m/s. **Figs. 2-4** show the comparison of non-dimensional u, h and z as functions of x computed by three different approaches: the first, second approximations and the exact solution by numerical computation for Case 1.

It is found that both u and z increase while h decreases in the upstream direction. **Fig. 4** shows the upward-concave bed profile in contrast to the downward-concave bed profile that appears in the erosional process. The upward-concave profiles imply that the bed slope is reduced from upstream to downstream and the corresponding flow velocity decreases, which causes the deposition of sediment transported from upstream. This corresponds well to various types of depositional phenomena such as alluvial fan. Since the second approximation gives the close results with the numerical computation in the sufficient upstream length (x = 100 is around 23 km in dimensional value), the second approximation is employed in the further analysis. In **Fig. 5**, the comparison between Case 1 (lower z_{ds}, higher σ) and Case 2 (higher z_{ds}, lower σ) is shown. It is found that higher migration speed yields steeper bed profile.

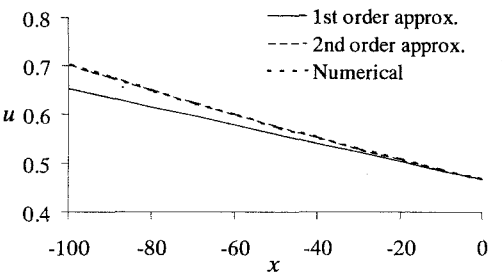

Fig. 2 Profile of non-dimensional u: comparison between 1st, 2nd approximation and numerical computation for Case 1.

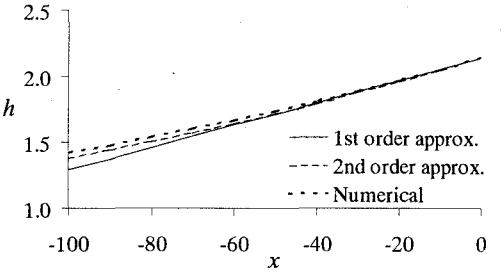

Fig. 3 Profile of non-dimensional h: comparison between 1st, 2nd approximation and numerical computation for Case 1.

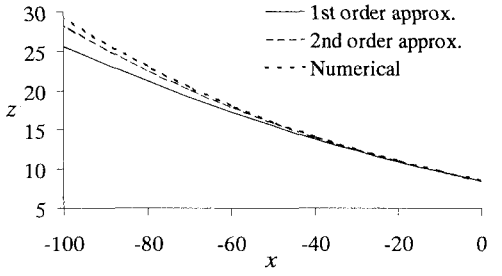

Fig. 4 Profile of non-dimensional z: comparison between 1st, 2nd approximation and numerical computation for Case 1.

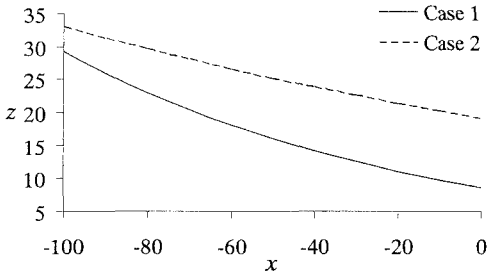

Fig. 5 Profile of non-dimensional z: comparison between Case 1 (higher σ) and Case 2 (lower σ).

4. THE TWO-DIMENSIONAL PROBLEM

(1) Linearization

The following perturbation is introduced at the delta front:

$$z = z_0 + ae^{\omega t} z_1(x)\cos ky + O(a^2) \tag{28}$$

where subscript 0 and 1 means the base state and the first order of the perturbation respectively, a, k and ω are the amplitude, wave number and growth rate of perturbation, respectively. Correspondingly, the other variables are expanded as

$$u = u_0 + ae^{\omega t} u_1(x)\cos ky + O(a^2) \tag{29}$$

$$v = ae^{\omega t} v_1(x)\sin ky + O(a^2) \tag{30}$$

$$h = h_0 + ae^{\omega t} h_1(x)\cos ky + O(a^2) \tag{31}$$

Substituting the above equations into Eqs.(14)-(17), at $O(a)$, we have

$$u_0\frac{du_1}{dx} + \frac{dh_1}{dx} + \frac{dz_1}{dx} + \left(\frac{2u_0}{h_0} + u_0'\right)u_1 - \frac{u_0^2}{h_0^2}h_1 = 0 \tag{32}$$

$$u_0\frac{dv_1}{dx} + \frac{u_0}{h_0}v_1 - kh_1 - kz_1 = 0 \tag{33}$$

$$h_0\frac{du_1}{dx} + u_0\frac{dh_1}{dx} + h_0'u_1 + kh_0v_1 + u_0'h_1 = 0 \tag{34}$$

$$3u_0^2\frac{du_1}{dx} - \sigma\frac{dz_1}{dx} + 6u_0u_0'u_1 + ku_0^2v_1 + \omega z_1 = 0 \tag{35}$$

where prime denotes d/dx. Further manipulation of the above equations yields

$$\frac{du_1}{dx} = \frac{1}{C_1}\left[\frac{u_1}{h_0}(2\sigma u_0^2 - \sigma h_0h_0' + \sigma u_0' + 6u_0u_0') + k(-\sigma h_0 + u_0^3)v_1 - \frac{\sigma h_1}{h_0^2}(u_0^3 + h_0^2u_0') + \omega u_0 z_1\right] \tag{36}$$

$$\frac{dv_1}{dx} = -\frac{v_1}{h_0} + \frac{kh_1}{u_0} + \frac{kz_1}{u_0} \tag{37}$$

$$\frac{dh_1}{dx} = \frac{1}{C_1}\left[(-2\sigma u_0 + \sigma u_0h_0' + 3u_0^2h_0' - 6u_0' - \sigma h_0u_0')u_1 + k(\sigma + 2u_0)v_1 + \frac{h_1}{h_0}(\sigma u_0' + \sigma u_0^2 + 3u_0u_0') - \omega h_0 z_1\right] \tag{38}$$

$$\frac{dz_1}{dx} = \frac{1}{C_1}\left[\frac{3u_1}{h_0}(2u_0^4 - u_0h_0' + 2h_0u_0' - u_0^2u_0') - k(2u_0 + u_0^4)v_1 - \frac{3h_1}{h_0^2}(u_0^5 + u_0') + \omega(h_0 - u_0^2)z_1\right] \tag{39}$$

where $C_1 = \sigma h_0 - u_0^2(\sigma + 3u_0)$

(2) Boundary conditions

In order to solve Eqs. (36)-(39) which is composed of 5 variables u_1, v_1, h_1, z_1 and ω, five boundary conditions are needed. Far upstream from the delta front, the perturbations are assumed to disappear; thus we have

$$u_1 = v_1 = h_1 = z_1 = 0 \quad \text{as} \quad x \to -\infty \tag{40}$$

The scrutiny of Eqs. (36)-(39) reveals, however, that if three of the above conditions (40) are imposed, the fourth one is satisfied by itself. Thus, in reality, only three independent boundary conditions are specified by Eq. (40).

In the light of Eq. (28), z_1 must be normalized so as to satisfy the following condition at the origin:

$$z_1 = 1 \quad \text{at} \quad x = 0 \tag{41}$$

The condition at the downstream boundary of the flow domain is preserved in the present analysis. The downstream boundary, however, is no longer located precisely at $x = 0$ due to the perturbations. The following condition holds:

$$h + z = \frac{\tilde{H}_{off}}{\tilde{H}_c} \quad \text{at} \quad x = a\chi e^{\omega t}\cos ky \tag{42}$$

where χ is a constant and the quantity $a\chi e^{\omega t}\cos ky$ denotes the perturbed position of the delta front in response to the perturbations Eqs.(28)-(31). Substituting Eqs.(28)-(31) into (42) and reducing, at $O(a)$, it is found that

$$\chi h_0' + \chi z_0' + h_1 + z_1 = 0 \quad \text{at} \quad x = 0 \tag{43}$$

and the quantity of $a\chi e^{\omega t}\cos ky$ can be described by the difference of the migration speeds; thus

$$\frac{u^3}{z} = \frac{\partial(\sigma t + a\chi e^{\omega t}\cos ky)}{\partial t} \quad \text{at} \quad x = a\chi e^{\omega t}\cos ky \tag{44}$$

Expanding Eq.(44) and reducing, at $O(a)$ in a it is found that

$$\frac{3u_0^2 u_1}{z_0} - \frac{u_0^3 z_1}{z_0^2} + \left(\frac{3u_0^2 u_0'}{z_0} - \frac{u_0^3 z_0'}{z_0^2}\right)\chi = \omega\chi \tag{45}$$

Therefore, substuting Eq.(45) into (43) and reducing, the fifth boundary condition is obtained:

$$3\frac{u_0^2 u_1}{z_0} + h_1\left(\frac{u_0^3 z_0' - 3u_0^2 u_0' z_0 + \omega z_0^2}{z_0^2(h_0' + z_0')}\right) + z_1\left(\frac{-u_0^3 h_0' - 3u_0^2 u_0' z_0 + \omega z_0^2}{z_0^2(h_0' + z_0')}\right) = 0 \tag{46}$$

Equations (36)-(39) have solutions satisfying the boundary conditions (40)-(41) and (46) only for particular values of ω. It is apparent that we cannot obtain the analytical solutions, so the equations are solved numerically using the relaxation method for two-point boundary value problems outlined in Press *et al.*[7]

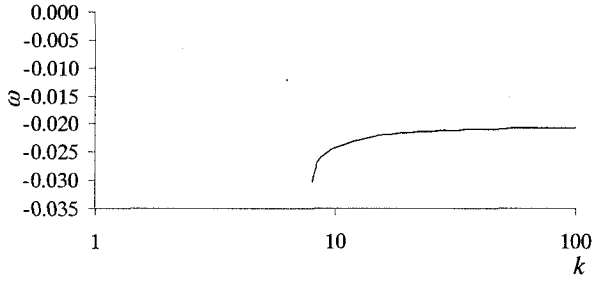

Fig. 6 The growth rate ω as a function of k for Case 1.

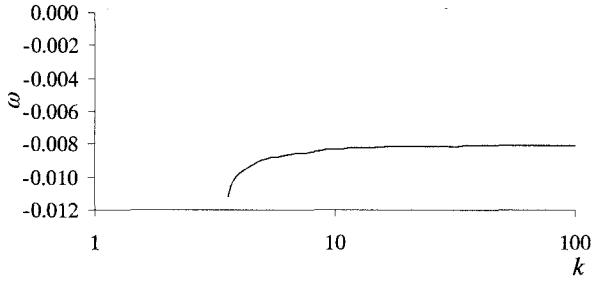

Fig. 7 The growth rate ω as a function of k for Case 2.

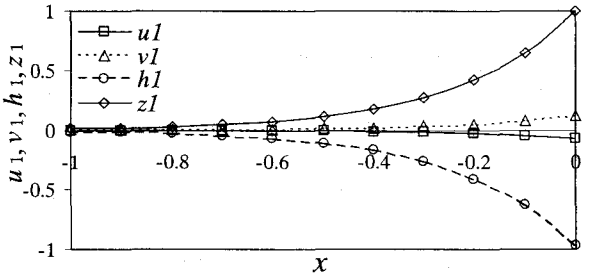

Fig. 8 Plots of u_1, v_1, h_1 and z_1 for Case 1 and $k = 10$.

5. RESULTS AND DISCUSSION

(1) Stability from the perturbation

Figs. 6 and **7** show the growth rate ω as a function of wavenumber k for Cases 1 and Case 2 (higher z_{ds}, lower σ) in **Table 1**, respectively. In both cases, it is found that the growth rate ω approaches asymptotically to a constant negative value in the range of large k, while we cannot calculate the values of ω in the range of small k because of the rapid decrease of ω. Growth rate ω decreases rapidly around $k = 9$ (wavelength $\tilde{L} = 151$ m.) for Case 1 and $k = 4$ ($\tilde{L} = 340$ m.) for Case 2. Comparing the value of ω between Case 1 (lower z_{ds}, higher σ) and Case 2 (higher z_{ds}, lower σ), we found that the growth rate ω in Case 2 is higher than that in Case 1, and the abrupt drop of the growth rate ω is seen in the range of smaller wave number k. Since $\sigma = u_{ds}^3 / z_{ds}$ and u_{ds} is unchanged in both cases, we can conclude that higher z_{ds} provide higher ω. The profiles of u_1, v_1, h_1 and z_1 for Case 1

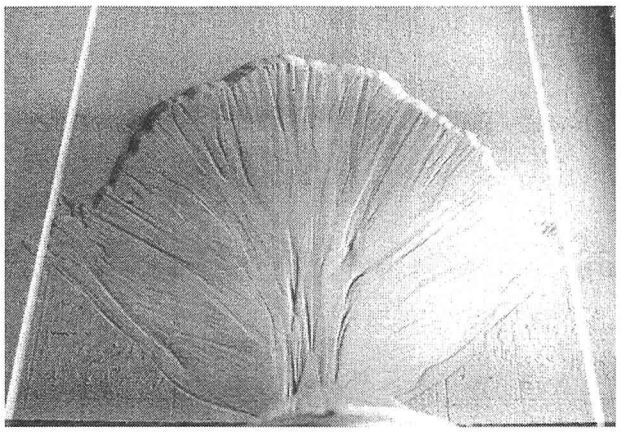

Fig. 9 Experiment on bedload-dominated fan.

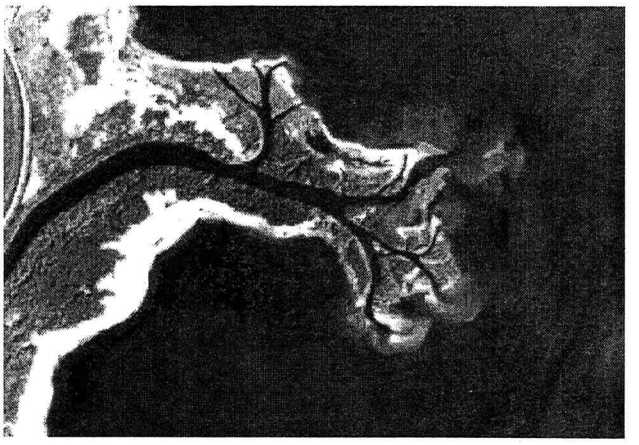

Fig. 10 River mouth delta in Abashiri Lake.

with k = 10 are shown in **Fig. 8**. All of them decrease and approach to zero at the far upstream.

Though we try various parameters in the model, it is always found that the growth rate ω is negative in any value of k. This implies that the bedload-dominated alluvial deltas are stable to the perturbation provided at the delta front.

(2) Roles of sediment transport processes

Fig.9 shows a fan delta formed in an experiment performed by one of the authors in Tokyo Institute of Technology, in which only bedload was observed. In the experiment, the delta is observed to develop concentrically keeping its round shape of delta front. Even though shallow channels are formed on the delta surface temporarily one after another, they are unstable to disappear shortly. The results obtained in this analysis correspond to the fact that bedload-dominated deltas have a stable front shape that tends to keep its parallel or round shape. Therefore, elongate deltas described subsequently cannot be formed with coarse sediment.

Fig.10 shows the river mouth delta formed in the Abashiri Lake, which is a typical example of the elongate delta as is the case with Mississippi delta. At the river mouth, the accumulation of huge quantities of sediment both suspended and bedload allows the delta front to extend into the lake[8]. It is suggested that the suspended sediment might be an important factor of the channel inception of the elongate delta, which should be further studied in the future.

6. CONCLUSIONS

A linear stability analysis is performed to investigate the incipient channelization on the deposition process of bedload-dominated alluvial deltas with the use of downstream-driven theory. In the one-dimensional base state, the bed profile presents upward-concave characteristic in contrast to the erosion processes of the previous researches, which the downward-concave bed profiles were found. Then, the linear analysis indicates that the bedload-dominated alluvial deltas are always stable or it can say that the plain migration propagates without the presence of the channels at its downstream. The phenomenon of bedload-dominated fan is well presented for the case of our present model. It also suggests that the presence of the suspended sediment should be an essential factor to cause the channelization in the alluvial deltas.

REFERENCES

1) Nemec, W.: Deltas – remarks on terminology and classification. In: A. Collela and D. B. Prior (Editors), *Coarse-Grained Deltas*, Int. Assoc. Sedimentol. Spec. Publ. No. 10, pp. 3-12, 1990.
2) Einsele, G.: Event deposits: the role of sediment supply and relative sea-level changes – overview, *Sediment. Geol., Vol. 104*, pp. 11-37, 1996
3) Izumi, N. and Parker, G.: Linear stability of channel inception: downstream-driven theory, *J. Fluid Mech., Vol. 419*, pp. 239-262, 2000.
4) Dey, A., Kitamura, K. and Tsujimoto, T.: Perturbations along headcut and their effects on gully formation, *J. Hyd., Coast. and Env. Eng. Vol. 677/II-55*, JSCE, pp. 205-213, 2001.
5) Izumi, N.: Formation of submarine canyons, *2nd Proc. RCEM, IAHR*, Japan, pp.71-80, 2001.
6) Izumi, N. and Ikeda, S.: Self-preserving longitudinal profile of one-dimensional delta, *Annual Journal of Hydraulic Engineering*, Vol. 40, pp. 915-920, 1996.
7) Press, H. P., Teukolsky, S. A., Vetterling, W. T. and Flannery, B. P.: *Numerical Recipes in FORTRAN*, 2nd Edn. Cambridge University Press, 1992.
8) Date, M., Izumi, N. and Tanaka, H.: Deltaic processes at the river mouth of the Abashiri river, *Annual Journal of Hydraulic Engineering*, Vol. 42, pp. 1129-1134, 1998.

(Received September 30, 2002)